Infection, Genetics and Evolution 103 (2022) 105326

Contents lists available at ScienceDirect

Infection, Genetics and Evolution

journal homepage: www.elsevier.com/locate/meegid

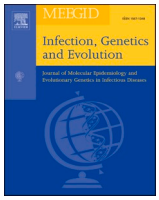

The genome and phylogenetic analyses of tit siadenoviruses reveal both a novel avian host and viral species

Ákos Gellért [a], Mária Benkő [a], Balázs Harrach [a], Martin Peters [b], Győző L. Kaján [a,*]

[a] Veterinary Medical Research Institute, Eötvös Loránd Research Network, 1581 Budapest, P.O. box 18, Hungary
[b] Chemical and Veterinary Investigation Office Westphalia, Zur Taubeneiche 10-12, 59821 Arnsberg, Germany

ARTICLE INFO

Keywords:
Complete genome
Eurasian blue tit
Great tit
Novel species
Siadenovirus
Sialidase

ABSTRACT

In both a Eurasian blue tit (*Cyanistes caeruleus*) and a great tit (*Parus major*), found dead in North Rhine-Westphalia, Germany, intranuclear inclusion bodies were observed in the kidneys during the histologic examination. Siadenoviruses were detected in both samples, and the nucleotide sequence of the partial DNA polymerase, obtained from the blue tit, was almost identical with that of great tit adenovirus type 1, reported from Hungary previously. The sequence, derived from the German great tit sample was more similar to great tit adenovirus 2, yet divergent enough to forecast the possible establishment of a novel viral type and species. Therefore, the complete genome was subjected to next generation sequencing. The annotation revealed a typical siadenoviral genome layout, and phylogenetic analyses proved the distinctness of the novel virus type: great tit adenovirus 3. We propose the establishment of a new species (*Siadenovirus carbocapituli)* within the genus *Siadenovirus* to contain great tit adenovirus types 2 and 3. As both of the newly-detected viruses originated from histologically confirmed cases, and several siadenoviruses have been associated with avian nephritis earlier, we assume that the renal pathology might have been also of adenoviral origin. Additionally, we performed structural studies on two virus-coded proteins. The viral sialidase and the fiber knob were modeled using the AlphaFold2 program. According to the results of the sialic acid docking studies, the fiber trimer of the new great tit adenovirus 3 binds this acid with good affinity. As sialic acid is expressed in the kidney, it can be hypothesized that it is used during the receptor binding and entry of the virus. Strong binding of sialic acid was also predictable for the viral sialidase albeit its enzymatic activity remains disputable since, within its catalytic site, an asparagine residue was revealed instead of the conserved aspartic acid.

1. Introduction

Adenoviruses are double-stranded DNA viruses. The major capsid proteins of their icosahedral capsids are the hexon, the penton base and the fiber (Gallardo et al., 2021). Birds in general can be infected by the members of three adenoviral genera: *Avi-*, *At-* and *Siadenovirus* (Benkő et al., 2022). Economically important avian adenoviral diseases are in chickens the inclusion body hepatitis, hepatitis-hydropericardium syndrome, gizzard erosion (caused by aviadenoviruses), egg drop syndrome (atadenovirus) and avian adenovirus splenomegaly (siadenovirus). The latter one is caused by the etiological agent of the turkey hemorrhagic enteritis. Furthermore, adenoviruses can be detected from a wide variety of domestic and wild birds as well (Harrach et al., 2019), including passeriforms (Athukorala et al., 2020; Harrach et al., 2022; Kovács et al., 2010; Phalen et al., 2019; Rinder et al., 2020; Vaz et al., 2020).

In 2020, increased mortality has been observed among tits in Germany (Fischer et al., 2021). The birds have been pathomorphologically and microbiologically investigated in governmental veterinary investigation laboratories using a broad diagnostic panel. Organ samples (heart, lung, liver, spleen, kidney, small intestine) have been examined microbiologically as described by Merbach et al. (2019). Combined oropharyngeal and cloacal swabs have been tested for avian influenza using the virotype Influenza A RT-PCR Kit (Indical Bioscience), central nervous system, liver, spleen and lung samples for Usutu and West Nile virus (Ziegler et al., 2022), and liver samples for *Chlamydia* sp. using PCR (Pantchev et al., 2009). In general, it has been found that *Suttonella ornithocola* had played an important role in the tits' mortality, but this bacterium may have been combined with other sporadic and/or endemic causes (Fischer et al., 2021). For example, for both a Eurasian blue tit (*Cyanistes caeruleus*) and a great tit (*Parus major*), *Suttonella*

* Corresponding author.
E-mail address: kajan.gyozo@vmri.hu (G.L. Kaján).

https://doi.org/10.1016/j.meegid.2022.105326
Received 26 March 2022; Received in revised form 10 June 2022; Accepted 26 June 2022
Available online 30 June 2022

ornithocola has not been cultured from any organ samples, as well as both tits have been negative for *Chlamydia* sp., avian influenza, Usutu and West Nile virus. However, for both tits, intranuclear inclusion bodies – consistent with adenoviruses – have been observed during the histologic investigation of the kidneys using light microscopy. The two samples have been tested using a broad-spectrum adenovirus-targeting PCR (Wellehan et al., 2004)and have yielded positive results. The sequences of the PCR products (NCBI GenBank accession numbers: MW508337 and MW508338 for the Eurasian blue tit and great tit adenovirus, respectively) were compared to that of the reference strains' DNA polymerases from all accepted adenoviral species. For the great tit adenovirus, the highest amino acid sequence identity was 76.4% compared to the chinstrap penguin adenovirus 2 (species *Penguin siadenovirus A*) (Lee et al., 2014). Thus, a complete genome sequencing was conducted on the strain, to investigate the possibility of whether it represents a novel siadenovirus species.

2. Material and methods

2.1. Origin of samples, pathology and histology

A female Eurasian blue tit (S425/20) and a male great tit (S478/20), both adults, were found dead during a mortality event observed in tits at two different locations in North Rhine-Westphalia, Germany (Fischer et al., 2021). Both tits were necropsied, and for histopathology, representative samples from the brain, lung, heart, liver, spleen, kidney and skeletal muscle were collected, fixed in 10% neutral-buffered formalin, embedded in paraffin wax, sectioned at 3 μm and stained with hematoxylin and eosin.

2.2. DNA extraction and pan-adenovirus PCR

Total DNA was extracted from frozen kidney samples of the Eurasian blue tit and the great tit using the NucleoSpin DNA RapidLyse kit (Macherey-Nagel), and the adenoviruses were detected using a pan-adenovirus PCR (Kaján, 2016; Kaján et al., 2011; Wellehan et al., 2004). Products were Sanger sequenced in both directions.

For the complete genome sequencing of the great tit adenovirus, about 1 mm^3 kidney sample was homogenized in phosphate-buffered saline using stainless steel bead disruption on a TissueLyser LT (Qiagen). After three times freeze-thawing, a 95 °C water bath for 10 min and finally an ultrasonic water bath at room temperature for 15 min, the homogenate was centrifuged at 5.000 ×*g* for 5 min, and the supernatant again at 13.000 × *g* for 5 min. To eliminate non-viral DNA, the supernatant was treated with DNA Degradase Plus (Zymo Research) for 2 h at 37 °C, then the DNase was deactivated at 70 °C for 20 min. From this solution, DNA was extracted using the NucleoSpin DNA RapidLyse kit (Macherey-Nagel).

2.3. Complete genome sequencing, assembly and phylogenetic analyses

The DNA, extracted for complete genome sequencing purposes from the great tit kidney, was sequenced using Illumina MiSeq equipment by a commercial provider. De novo assembly of the reads using the Geneious assembler resulted in a 26,099-bp-long contig, then all reads were mapped to this. To the final consensus sequence, genome annotations were transferred from the chinstrap penguin adenovirus 2 using Geneious and these were manually checked and edited.

The phylogenetic tree was inferred based on deduced DNA polymerase amino acid sequences. To aid proper phylogenetic placement, the complete coding sequences were used where available (e.g., strain S478/20 and from other complete genomes), and these were aligned with the partial coding sequences (e.g., strain S425/20). The alignment was conducted using the MAFFT G-INS-I algorithm (Katoh and Standley, 2013), and was edited manually. The rtREV+I+G evolutionary model was applied, selected using ModelTest-NG v0.1.5 (Darriba et al., 2020). The best phylogenetic tree was chosen from 300 replicates inferred using RAxML-NG v1.0.1, and the robustness of the tree was determined with a non-parametric bootstrap calculation using 1000 repeats (Kozlov et al., 2019). The transfer bootstrap expectation values were applied to the tree (Lemoine et al., 2018). The phylogenetic tree was visualized using MEGA 7, and it was rooted on the midpoint, and bootstrap values were given as percentages if they reached 75% (Kumar et al., 2016).

To determine the amino acid sequence identity of the tit strains compared to different adenoviral species, a pairwise sequence identity analysis was also conducted based on both the complete and the partial DNA polymerase sequences using the Sequence Demarcation Tool v1.2 (Muhire et al., 2014).

2.4. In silico protein modeling

The entire putative sialidase and fiber knob (amino acids 344–489) were modeled from the great tit adenovirus (S478/20) using AlphaFold2, a deep learning automatic protein structure modeling software (Jumper et al., 2021). Additionally, the psittacine adenovirus 2 sialidase (QXX30959) structure was also modeled (Surphlis et al., 2022). This reference siadenoviral sialidase was the closest blastp hit to the great tit adenovirus sialidase. Five models were generated for each protein, evaluated using the protein structure quality assignment module of AlphaFold2 and the best further refined using the Schrödinger Suite to eliminate the steric conflicts between the side-chain atoms (Schrödinger, 2021). The crystal structure of the human adenovirus 26 fiber trimer complexed with sialic acid (Protein Data Bank [PDB] ID: 6QU8) was used to generate the fiber knob trimer from the monomeric model (Baker et al., 2019). Electrostatic surface potential maps were calculated using the Adaptive Poisson-Boltzmann Solver version 1.3 using the linearized Poisson-Boltzmann method with a dielectric constant of 78.0 and 2 for the water solvent and the protein core, respectively (Baker et al., 2001). The partial charges in the electrostatic potential were calculated using PDB2PQR (Baker et al., 2001). Molecular graphics were created using VMD version 1.9.3 (Humphrey et al., 1996).

2.5. Sialic acid docking

To check the sialic acid affinity of the great tit adenovirus fiber knob trimer and the putative sialidase enzyme, the Glide ligand docking module of the Schrödinger Suite was used (Schrödinger, 2021). The LigPrep module was used to generate 32 initial conformations from sialic acid (PDB ligand: SLB) and this conformation set was used as the ligand input for the docking calculations. The previous human adenovirus fiber structure (PDB ID: 6QU8) was chosen as a reference for the fiber's binding, whereas sialidase26, a bacterial sialidase (PDB ID: 6MYV) (Zaramela et al., 2019), and the psittacine adenovirus 2 sialidase model were selected for the putative sialidase. The docking grids were created using the Receptor Grid Generator module of Schrödinger Glide, and then the previously generated sialic acid conformation library was docked to the reference and the modeled structures with standard precision. The best-ranking docking positions were used for comparisons. Finally, an alignment of the putative viral sialidase enzyme was conducted with four additional siadenoviral sialidases using the MAFFT G-INS-I algorithm (Katoh and Standley, 2013).

3. Results

3.1. Pathology and histology

The main pathological finding and cause of death in the Eurasian blue tit was a blunt trauma with severe hemorrhages in the liver and the lungs. Macroscopically, the spleen and kidneys did not present significant findings. Histologically, other organs yielded a negative result, but large amphophilic intranuclear inclusion bodies were detected in the renal tubular epithelial cells which showed degeneration and necrosis

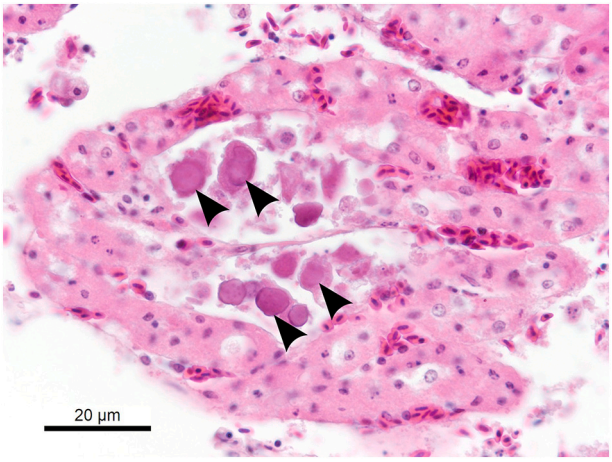

Fig. 1. Renal histology of the Eurasian blue tit. Amphophilic intranuclear adenovirus inclusion bodies (arrowheads) within the necrotic renal tubular epithelium. Hematoxylin and eosin stain, bar = 20 μm. (For interpretation of the references to colour in this figure legend, the reader is referred to the web version of this article.)

(Fig. 1). In the great tit, the spleen was severely enlarged. Histologically, mild lymphocytic nephritis was observed with large amphophilic intranuclear inclusion bodies in the tubular epithelial cells (Fig. 2) besides unidentified intracytoplasmic agents in groups within the cytoplasm of muscular vessel endothelial cells and perivascular macrophages in the skeletal muscle sections. Other organs did not reveal any pathohistological lesions in either bird.

3.2. Phylogenetic analyses

The phylogenetic tree reconstruction is displayed in Fig. 3. Both tit adenoviruses clustered into the genus *Siadenovirus*. On the analyzed partial DNA polymerase gene sequence, the Eurasian blue tit adenovirus (S425/20) shared 100% nucleic acid identity with the great tit adenovirus 1 (species *Great tit siadenovirus A*) virus strain identifier 48820 (Rinder et al., 2020), and a single nucleotide difference was observed compared to the prototype strain 5957/SZ (Kovács et al., 2010), but this caused a silent mutation only. The great tit adenovirus strain S478/20 clustered with the great tit adenovirus 2 virus strain identifier 49056 (Rinder et al., 2020), and the amino acid sequence identity of the two partial DNA polymerase sequences was 89.9%. Thus, strain S478/20 is

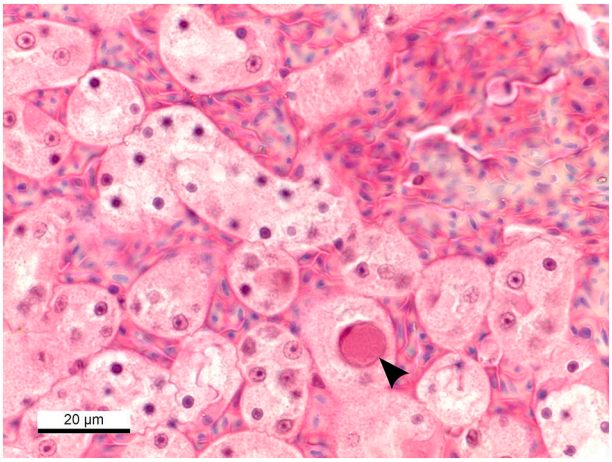

Fig. 2. Renal histology of the great tit. A large amphophilic intranuclear adenovirus inclusion body (arrowhead) within a tubular epithelial cell. Hematoxylin and eosin stain, bar = 20 μm.

proposed to be the reference strain of a novel type: great tit adenovirus 3. When the complete DNA polymerase amino acid sequence of strain S478/20 was compared to members of the genus *Siadenovirus*, the highest measured sequence identity was 65.3% compared to great tit adenovirus 1 (ACW84422, species *Great tit siadenovirus A*) (Kovács et al., 2010), whereas 76.4% sequence identity was measured based on the partial DNA polymerase amino acid sequence compared to chinstrap penguin adenovirus 2 (Lee et al., 2014).

3.3. Genome sequence

The complete genome sequence obtained from the sample S478/20 was found to be 26,075 bp long with a G + C-content of 38.4%. The read coverage minimum was 19, the mean was 117.8, the read coverage's standard deviation was 59.8, and the confidence mean of bases was 1896.4. A typical siadenoviral genome layout was revealed with 25 protein-coding sequences and 37-bp-long inverted terminal repeats. On the right genomic end, two open reading frames were annotated on the leftward-transcribed (*l*) genomic strand. The predicted proteins shared 36.6% and 32.1% amino acid sequence identity with hypothetical proteins (QXX30970, QZW33711) of the psittacine adenovirus 2, respectively (Athukorala et al., 2021; Sarker, 2021; Surphlis et al., 2022).

3.4. Fiber structure and function

Despite the high evolutionary distance from other adenovirus fibers with already determined structure, the AlphaFold2, a deep learning automatic protein structure modeling method (Jumper et al., 2021), could generate a good quality model for the fiber knob domain: the average predicted local-distance difference test of the residues was 81.6. The fiber knob domain of the newly described great tit adenovirus 3 fiber is 39 amino acids shorter than the chosen reference human adenovirus 26 fiber knob domain: 146 instead of 185 amino acids. The beta-barrel fold was well conserved but significant differences were identified in the loop structures (Fig. 4). Sialic acid docking scores and binding energies are summarized in Table 1.

3.5. Putative sialidase structure and function

The putative sialidase of great tit adenovirus 3 shows high sequence similarity and structural homology to the bacterial sialidase enzyme used as reference (PDB ID: 6MYV) (Zaramela et al., 2019). Hence, the models, generated by AlphaFold2 had good protein structure quality values: the averages of the predicted local-distance difference tests of the residues were 79.2 and 83.0 for the great tit adenovirus and the psittacine adenovirus 2 sialidase, respectively. The docking calculation predicted that the sialidase of this newly found siadenovirus most likely binds oligosaccharides with sialic acid ending (Fig. 5 and Table 1). However, the bound sialic acid is not in an orientation where the glycosidic hydroxyl group is close to the enzymatic catalytic side chain that performs the nucleophilic attack. Moreover, in this enzymatic catalytic site, an asparagine residue (Asn108) was revealed instead of the conserved aspartic acid (Figs. 5 and 6). Furthermore, in the other two modeled sialidase enzymes, the carboxylic acid group of the sialic acid is coordinated by three conserved arginines (bacterial: Arg203, Arg414 and Arg478; psittacine: Arg83, Arg251 and Arg280; Fig. 5D and F), allowing the correct orientation of the glycosidic hydroxyl group to the catalytic aspartate side chain. In contrast, the great tit adenovirus sialidase was mutated in two out of these three sites: Thr83 and Asn350 (Figs. 5E and 6).

4. Discussion

Hereby, we present the complete genome of a great tit siadenovirus, and also a novel host species, Eurasian blue tit, for the previously described viral species *Great tit siadenovirus A*. The primary species

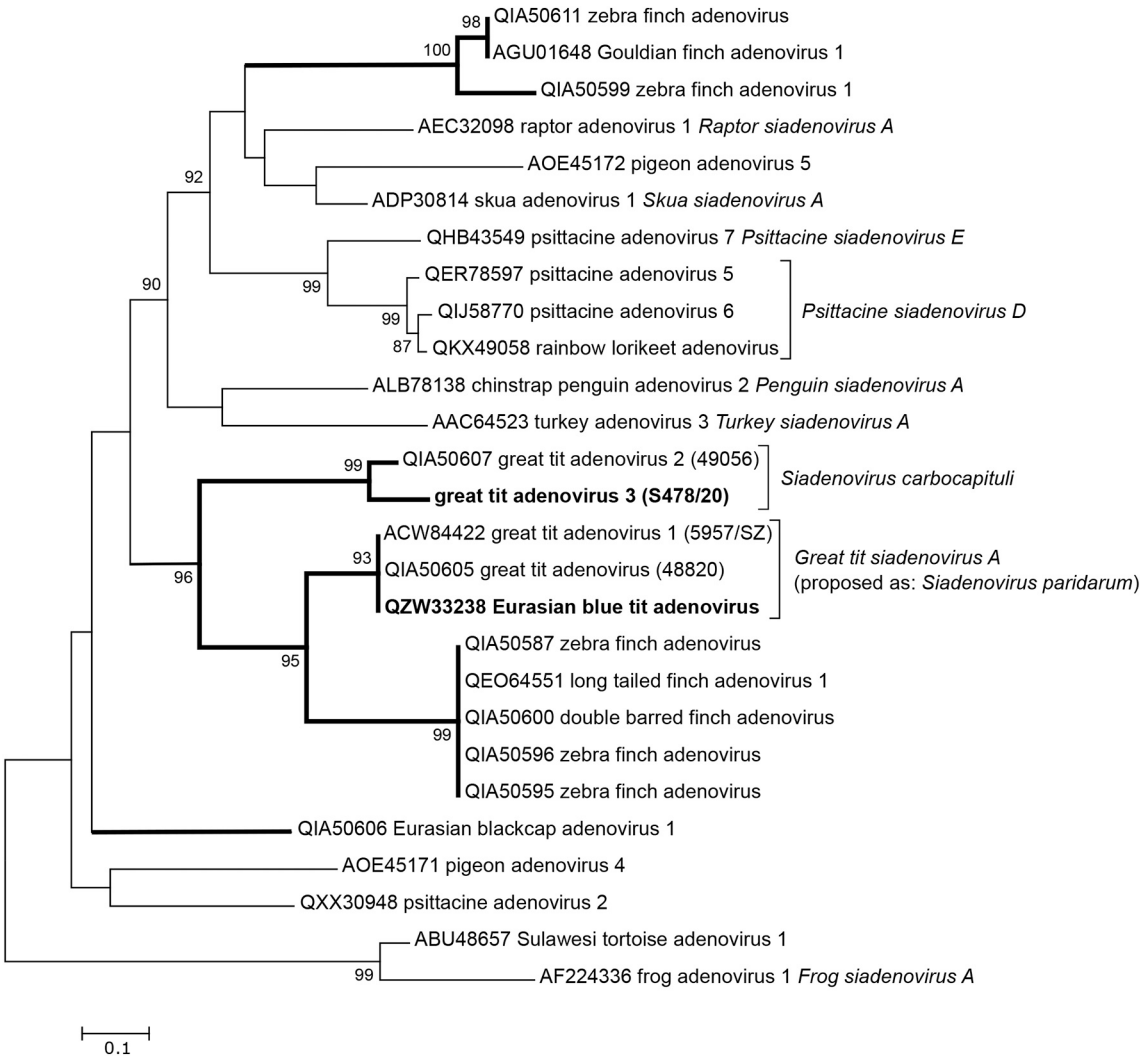

Fig. 3. Phylogenetic analysis of the Eurasian blue tit and the great tit adenovirus strains (S425/20 and S478/20, respectively) compared to siadenoviruses based on the viral DNA polymerase amino acid sequences. The analyzed great tit adenovirus 3 and Eurasian blue tit adenovirus strains are in bold, and branches of passeriform adenoviruses are thickened. For great tit adenovirus strains, the strain identifiers are also given in parenthesis.

demarcation criterion for siadenoviruses is 10–15% divergence on the DNA polymerase amino acid sequence (Benkő et al., 2022), and here 65.3% sequence identity was measured highest for the genome sequenced adenovirus. Thus, we propose the establishment of a novel species, named *Siadenovirus carbocapituli*, derived from the Hungarian name of the host species (széncinege, roughly translated: coal tit) and its head colour. The proposed virus species contains two types: great tit adenovirus 2 and 3, the former represented by virus strain identifier 49056 (Rinder et al., 2020), and the latter by strain S478/20. As the partial DNA polymerase-based amino acid sequence identity between the two types was 89.9%, and the two strains were detected from the same host species, distinct species were not proposed for the two strains. Though it must be stressed that the official primary species demarcation criterion is based on the complete derived amino acid sequence of the DNA polymerase, and here only a partial one was available from strain 49056, representing great tit adenovirus 2.

As binomial scientific names are required for all viral species names until 2023, hereby we propose a new name for the species *Great tit siadenovirus A* as well (Kovács et al., 2010): *Siadenovirus paridarum*, as a member strain had been detected previously from great tit and was detected now from a Eurasian blue tit, avian species that belong to the family Paridae.

Both detected and analyzed tit adenoviruses were siadenoviruses. However, recently, a passerine atadenovirus, tentatively named passerine adenovirus 1, has also been reported from an eastern spinebill (*Acanthorhynchus tenuirostris*) in Australia (Athukorala et al., 2020). As there are over 140 families and 6500 species in the order Passeriformes, we propose the renaming of this adenovirus type to eastern spinebill adenovirus 1.

Concerning the evolution of siadenoviruses, at least two viral clades are hypothesized to coevolve with passeriform birds. This hypothesis is based on the two observable monophyletic passeriform siadenovirus clades: the first one containing Gouldian and zebra finch strains (Joseph et al., 2014; Rinder et al., 2020); the second one great and Eurasian blue tit strains and zebra, long-tailed and double-barred finch strains furthermore (Kovács et al., 2010; Phalen et al., 2019). There is a single exception in the phylogenetic tree reconstruction: the Eurasian blackcap adenovirus 1 – though detected in a passeriform host – is not clustering into the mentioned two clades (Rinder et al., 2020).

Both of the newly-detected tit adenoviruses (S425/20 and S478/20) originated from histologically confirmed cases, and several siadenoviruses have been associated with avian nephritis earlier (Ballmann and Harrach, 2016; Joseph et al., 2014; Phalen et al., 2019), we assume that the renal pathologies might have been also of adenoviral origin. Although the exact pathogenicity levels of these viruses are unknown yet. Strain S478/20 (great tit adenovirus 3) was detected from a great tit

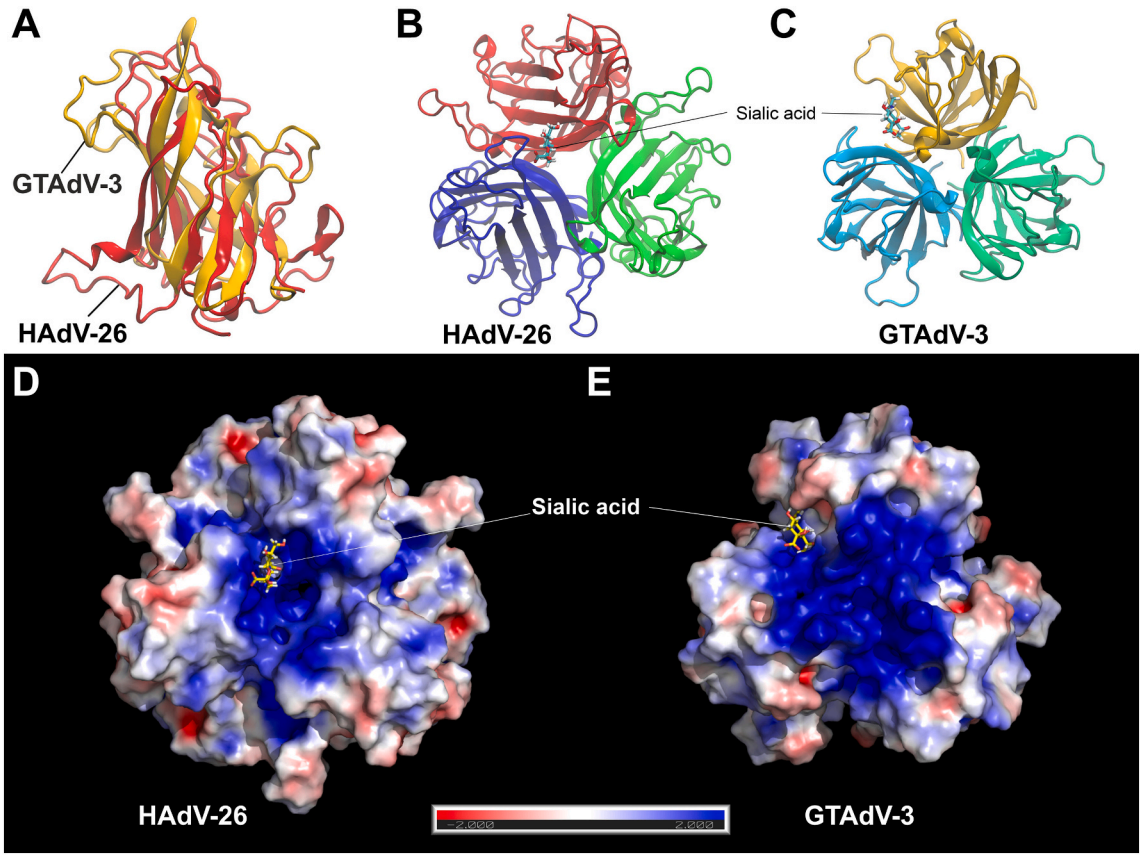

Fig. 4. Comparison of the great tit adenovirus 3 fiber knob structure with the reference human adenovirus 26 fiber knob. Superposition of the fiber knob monomers is in cartoon representation (A). Sialic acid binding sites are formed by two adjacent chains of fiber knobs in the reference human adenovirus fiber trimer (B) as well as in the great tit adenovirus fiber trimer (C). The electrostatic surface potentials of the trimeric fiber knobs (D and E), where red colour represents regions with a potential value below −2.0 kT, white represents 0.0 kT and blue above +2.0 kT. Abbreviations: GTAdV-3, great tit adenovirus 3; HAdV-26, human adenovirus 26. (For interpretation of the references to colour in this figure legend, the reader is referred to the web version of this article.)

Table 1
Sialic acid docking scores and energies to great tit adenovirus 3 fiber knob trimer and sialidase.

	Docking score	GlideScore	Emodel (kcal/mol)	Is sialic acid in a "catalytic" orientation?
Fiber knob trimer				
great tit adenovirus 3	−5.716	−5.716	−49.943	not relevant
human adenovirus 26 (6QU8)	−6.557	−6.557	−54.740	not relevant
Sialidase				
great tit adenovirus 3	−6.458	−6.458	−67.072	No
psittacine adenovirus 2	−6.352	−6.352	−63.500	Yes
bacterial (6MYV)	−7.579	−7.579	−80.353	Yes

A single sialic acid binding site was explored, though the adenovirus fiber knob trimers have three equivalent sialic acid binding sites. Only the best docking scores are presented in this table. Lower docking scores correspond to higher affinity. Protein data bank accession numbers are given in parenthesis for the reference structures.

with – besides the nephritis – enlarged spleen and an intramuscular infection (Fischer et al., 2021). A generally weak, perhaps immunosuppressed state can be hypothesized which supports the exacerbation of chronic illnesses; thus, a primary pathogenic role of the virus is questionable. On the other hand, strain S425/20 (classified as great tit adenovirus 1) was detected from a traumatized Eurasian blue tit, which died most possibly in an abrupt way without the possibility of chronic illnesses to exacerbate. Still, histopathologic findings, intranuclear inclusion bodies were detected in its renal cells. Thus, higher pathogenicity might be linked to great tit adenovirus 1 at least in Eurasian blue tits. This might be further supported by the fact, that this adenovirus type was detected from two distinct host species, the great and the Eurasian blue tit. Adenoviruses that have coevolved with their host species have a narrow host range – usually one species – and a low level of pathogenicity in general. Whereas adenoviruses with broader host ranges are often more pathogenic (Kaján et al., 2020).

The sequenced great tit adenovirus 3 strain showed relatively high sequence identity with the chinstrap penguin adenovirus 1 based on the partial DNA polymerase amino acid sequence. Still, this new genome does contain a sialidase enzyme encoding gene, a homolog of which is missing from the penguin siadenoviruses (Lee et al., 2014). Another gene content debate is that of the so-called ORF4 (open reading frame 4). This gene annotation had been omitted from the first complete siadenovirus genome of the frog adenovirus 1 in favor of the presumed hydrophobic protein (Davison et al., 2000). Later, the presence of ORF4 has been supported based on its conserved nature in several avian siadenoviral genomes (Kovács and Benkő, 2011; Park et al., 2012; Surphlis et al., 2022). The genome of the great tit adenovirus 3 supports its existence further, whereas no hydrophobic-protein-encoding open reading frames were detected. On the right genomic end, further two open reading frames were annotated. Both possess homologs in some psittacine siadenoviruses (QHB43567, QIJ58772, QXX30970, QXX30971,

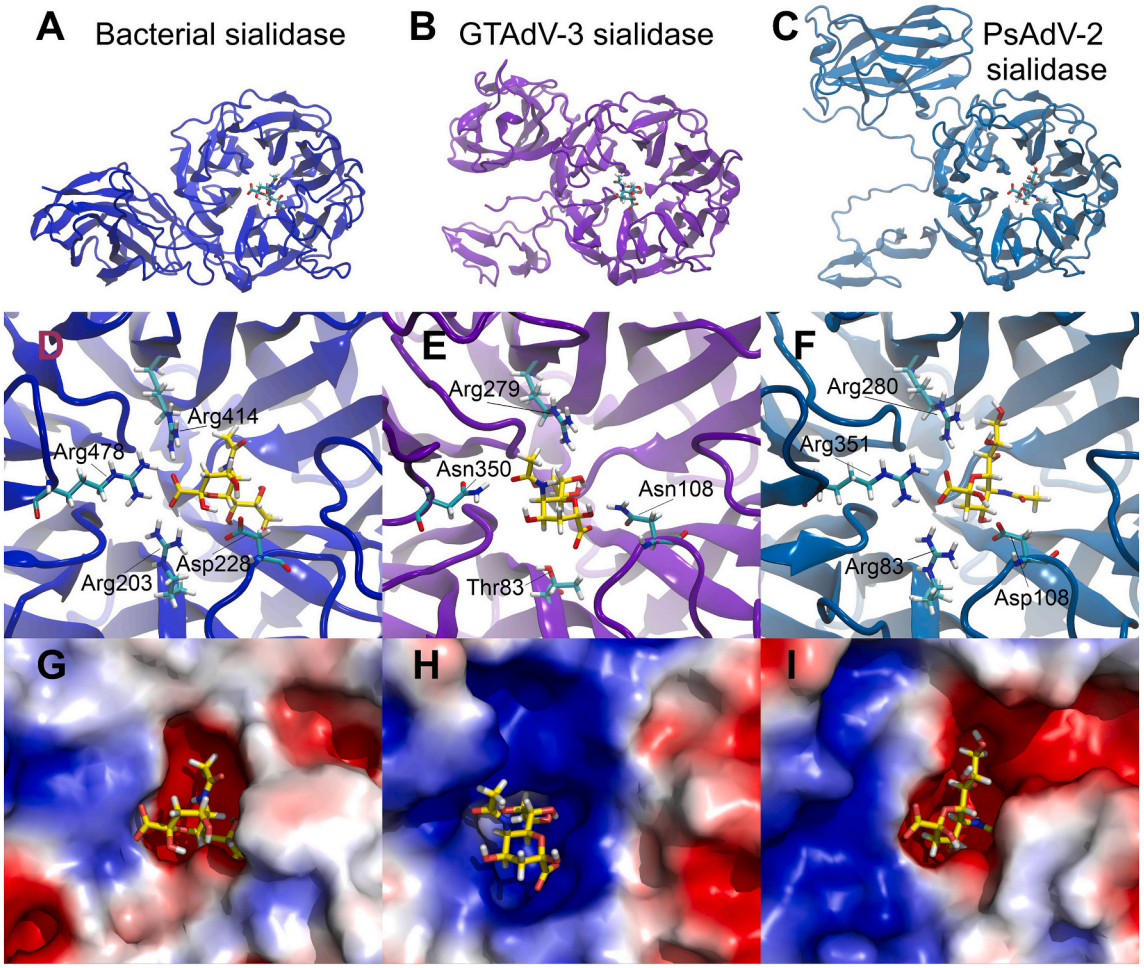

Fig. 5. Comparison of a bacterial (A), great tit adenovirus 3 (B), and the psittacine adenovirus 2 (C) sialidase structure in complex with sialic acid. The sialic acid binding sites are in the middle of the beta-propeller domains (D–F). The electrostatic surface views show a significant difference in the catalytic sites (G–I). On the electrostatic surface models, red colour represents regions with a potential value below −2.0 kT, white represents 0.0 kT and blue above +2.0 kT. Abbreviations: Arg: arginine; Asn: asparagine; Asp: aspartic acid; GTAdV-3, great tit adenovirus 3; PsAdV-2, psittacine adenovirus 2; Thr: threonine. (For interpretation of the references to colour in this figure legend, the reader is referred to the web version of this article.)

QZW33264, QZW33710, QZW33711) in the same genomic location and transcription direction (Athukorala et al., 2021; Sarker, 2021; Surphlis et al., 2022; Sutherland et al., 2019). Thus, the numbering of earlier described juxtapositioned open reading frames was continued, and these open reading frames were labeled as ORF9 and 10, respectively.

Well-conserved 22K and 33K genes were found in the conserved genomic position and orientation, but the common start codon of these genes was substituted by the triplet: ACC. If the next in-frame start codon was accepted, this meant that the gene of 22K was completely omitted, whereas the 33K gene had a single exon and the product was 36 amino acids long instead of 136. The sequence identity of the 22K gene product – with the alternative start codon accepted – was 59.2% (query cover: 98.96%) to the raptor adenovirus 1 homolog (AEC32102), whereas that of the 33K gene product was 55.6% (query cover: 95.59%) again to the raptor adenovirus 1 homolog (AEC32101) (Kovács and Benkő, 2011). These two genes are members of the conserved adenoviral gene cassette, which was found in every adenoviral genome to contain the same genes in conserved order and orientation (Davison et al., 2003). Also, both proteins have crucial roles in the viral life cycle (Guimet and Hearing, 2013; Wu et al., 2013, 2012); thus, their absence is not hypothesized. The triplet ACC was found functional as a start codon in algal chloroplasts (Chen et al., 1995), and non-AUG start codons are also used in eukaryotic cells (Kearse and Wilusz, 2017). Whether these genes are expressed using this alternative start codon requires further investigations.

Based on the sialic acid docking studies, the great tit adenovirus 3 fiber trimer binds sialic acid with good affinity similarly to several adenoviruses within species *Human mastadenovirus D* (Table 1) or *G* (Arnberg, 2012; Arnberg et al., 2002; Lenman et al., 2018, 2015). As sialic acid is expressed both in Madin-Darby canine kidney cells and in the human kidney (Babal et al., 1996; Burmeister et al., 2004), it is hypothesized that the sialic acid is used in viral receptor binding and entry. Strong binding is also hypothesized for the viral sialidase to sialic acid, but its enzymatic activity is disputable. Enzymological studies proved that only an acid-based nucleophilic attack can initialize the sialic acid cleavage mechanism (Withers et al., 1992), but the otherwise conserved aspartic acid is replaced by an asparagine residue in this catalytic site. Theoretically, the deamination of this asparagine side chain may yield an active enzyme again (Pries et al., 1995); still, the great tit adenovirus 3 sialidase homolog is probably inactive, as due to further mutations in the binding site the sialic acid cannot be bound in a proper, reactive orientation. However, experimental data may help to determine the exact activity level of this sialidase. Both the 22/33K alternative start codon and the sialidase active site sequence were confirmed using Sanger sequencing: no disagreements were found between Sanger and next-generation sequencing results.

Hereby we provide the complete genome sequence of great tit adenovirus 3 and propose that it is acknowledged as a member of a new

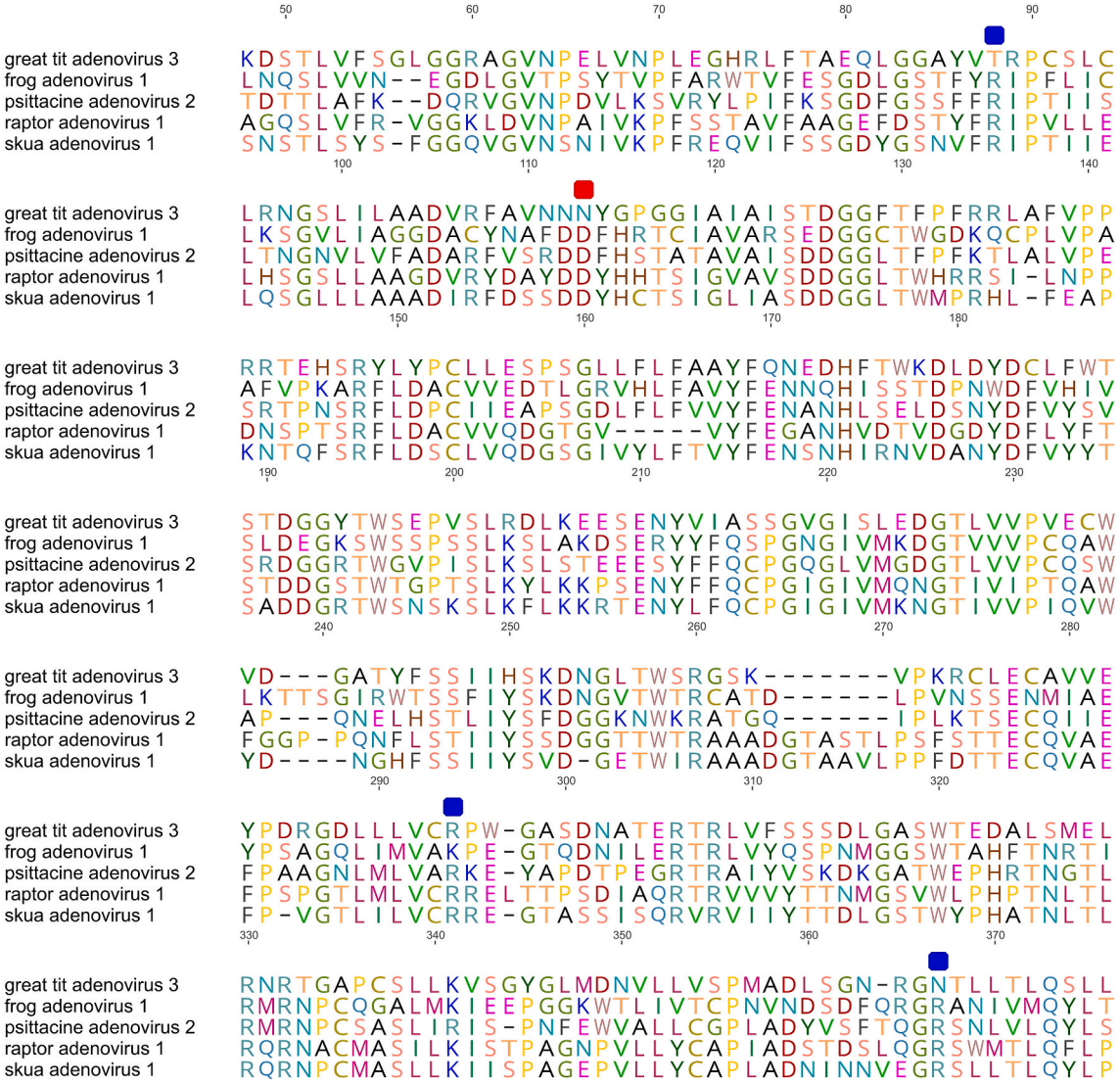

Fig. 6. Extract from the alignment of siadenoviral sialidases. The enzymatic catalytic site was highlighted with a red rectangle, and the enzymatic stabilizing sites with blue rectangles. In the great tit adenovirus 3, an asparagine (Asn/N 108) residue was revealed instead of the catalytic aspartic acid (Asp/D), conserved in other siadenoviruses, whereas two of the three stabilizing sites are also mutated: Thr/T 83 and Asn/N 350. Ordinals of amino acids are given according to great tit adenovirus 3 sialidase protein in this figure legend. See Fig. 5E for comparison. (For interpretation of the references to colour in this figure legend, the reader is referred to the web version of this article.)

adenovirus species: *Siadenovirus carbocapituli*. The previously described viral species *Great tit siadenovirus A* is proposed to be renamed *Siadenovirus paridarum*, and also a novel host species, the Eurasian blue tit, is described for one of its strains.

Funding

This research was partially funded by the National Research, Development and Innovation Office (grant number NN140356) and partially implemented with the support provided by the Ministry of Innovation and Technology of Hungary (legal successor: Ministry of Culture and Innovation of Hungary) from the National Research, Development and Innovation Fund, financed under the TKP2021-EGA-01 funding scheme of the National Research, Development and Innovation Office. The research of GLK is supported by the János Bolyai Research Scholarship of the Hungarian Academy of Sciences.

CRediT authorship contribution statement

Ákos Gellért: Formal analysis, Investigation, Visualization. **Mária Benkő:** Formal analysis, Writing – review & editing. **Balázs Harrach:** Resources, Writing – review & editing, Supervision, Funding acquisition. **Martin Peters:** Resources, Writing – review & editing. **Győző L. Kaján:** Conceptualization, Methodology, Formal analysis, Investigation, Writing – original draft, Visualization.

Declaration of Competing Interest

None.

Acknowledgments

Phylogenetic calculations were performed using computing resources provided by KIFÜ, Hungary. AlphaFold2 running was supported by the Ministry of Innovation and Technology National Research, Development and Innovation Office grant MILAB Artificial Intelligence

National Laboratory Program.

References

Arnberg, N., 2012. Adenovirus receptors: implications for targeting of viral vectors. Trends Pharmacol. Sci. 33, 442–448. https://doi.org/10.1016/j.tips.2012.04.005.

Arnberg, N., Kidd, A.H., Edlund, K., Nilsson, J., Pring-Akerblom, P., Wadell, G., 2002. Adenovirus type 37 binds to cell surface sialic acid through a charge-dependent interaction. Virology 302, 33–43. https://doi.org/10.1006/viro.2002.1503.

Athukorala, A., Forwood, J.K., Phalen, D.N., Sarker, S., 2020. Molecular characterisation of a novel and highly divergent passerine adenovirus 1. Viruses 12, 1036. https://doi.org/10.3390/V12091036.

Athukorala, A., Phalen, D.N., Das, A., Helbig, K.J., Forwood, J.K., Sarker, S., 2021. Genomic characterisation of a highly divergent siadenovirus (*Psittacine siadenovirus F*) from the critically endangered orange-bellied parrot (*Neophema chrysogaster*). Viruses 13, 1714. https://doi.org/10.3390/v13091714.

Babal, P., Slugen, I., Danis, D., Zaviacic, M., Gardner, W.A., 1996. Sialic acid expression in normal and diseased human kidney. Acta Histochem. 98, 71–77.

Baker, N.A., Sept, D., Joseph, S., Holst, M.J., McCammon, J.A., 2001. Electrostatics of nanosystems: application to microtubules and the ribosome. Proc. Natl. Acad. Sci. U. S. A. 98, 10037–10041. https://doi.org/10.1073/pnas.181342398.

Baker, A.T., Mundy, R.M., Davies, J.A., Rizkallah, P.J., Parker, A.L., 2019. Human adenovirus type 26 uses sialic acid–bearing glycans as a primary cell entry receptor. Sci. Adv. 5, eaax3567 https://doi.org/10.1126/sciadv.aax3567.

Ballmann, M.Z., Harrach, B., 2016. Detection and partial genetic characterisation of novel avi- and siadenoviruses in racing and fancy pigeons (*Columba livia domestica*). Acta Vet. Hung. 64, 514–528. https://doi.org/10.1556/004.2016.047.

Benkő, M., Aoki, K., Arnberg, N., Davison, A.J., Echavarría, M., Hess, M., Jones, M.S., Kaján, G.L., Kajon, A.E., Mittal, S.K., Podgorski, I.I., San Martín, C., Wadell, G., Watanabe, H., Harrach, B., 2022. ICTV Virus Taxonomy Profile: *Adenoviridae*. J. Gen. Virol. 103, 001721 https://doi.org/10.1099/jgv.0.001721.

Burmeister, W.P., Guilligay, D., Cusack, S., Wadell, G., Arnberg, N., 2004. Crystal structure of species D adenovirus fiber knobs and their sialic acid binding sites. J. Virol. 78, 7727–7736. https://doi.org/10.1128/JVI.78.14.7727-7736.2004.

Chen, X., Kindle, K.L., Stern, D.B., 1995. The initiation codon determines the efficiency but not the site of translation initiation in Chlamydomonas chloroplasts. Plant Cell 7, 1295–1305. https://doi.org/10.1105/TPC.7.8.1295.

Darriba, D., Posada, David, Kozlov, A.M., Stamatakis, A., Morel, B., Flouri, T., 2020. ModelTest-NG: a new and scalable tool for the selection of DNA and protein evolutionary models. Mol. Biol. Evol. 37, 291–294. https://doi.org/10.1093/molbev/msz189.

Davison, A.J., Wright, K.M., Harrach, B., 2000. DNA sequence of frog adenovirus. J. Gen. Virol. 81, 2431–2439. https://doi.org/10.1099/0022-1317-81-10-2431.

Davison, A.J., Benkő, M., Harrach, B., 2003. Genetic content and evolution of adenoviruses. J. Gen. Virol. 84, 2895–2908.

Fischer, L., Peters, M., Merbach, S., Eydner, M., Kuczka, A., Lambertz, J., Kummerfeld, M., Kahnt, K., Weiss, A., Petersen, H., 2021. Increased mortality in wild tits in North Rhine-Westphalia (Germany) in 2020 with a special focus on *Suttonella ornithocola* and other infectious pathogens. Eur. J. Wildl. Res. 67, 56. https://doi.org/10.1007/s10344-021-01500-7.

Gallardo, J., Pérez-Illana, M., Martín-González, N., Martín, C.S., 2021. Adenovirus structure: what is new? Int. J. Mol. Sci. 22, 5240. https://doi.org/10.3390/ijms22105240.

Guimet, D., Hearing, P., 2013. The adenovirus L4-22K protein has distinct functions in the posttranscriptional regulation of gene expression and encapsidation of the viral genome. J. Virol. 87, 7688–7699. https://doi.org/10.1128/JVI.00859-13.

Harrach, B., Tarján, Z.L., Benkő, M., 2019. Adenoviruses across the animal kingdom: a walk in the zoo. FEBS Lett. 593, 3660–3673. https://doi.org/10.1002/1873-3468.13687.

Harrach, B., Megyeri, A., Papp, T., Ursu, K., Boldogh, S.A., Kaján, G.L., 2022. A screening of wild bird samples enhances our knowledge about the biodiversity of avian adenoviruses. Vet. Res. Commun. https://doi.org/10.1007/s11259-022-09931-6.

Humphrey, W., Dalke, A., Schulten, K., 1996. VMD: visual molecular dynamics. J. Mol. Graph. 14, 33–38. https://doi.org/10.1016/0263-7855(96)00018-5.

Joseph, H.M., Ballmann, M.Z., Garner, M.M., Hanley, C.S., Berlinski, R., Erdélyi, K., Childress, A.L., Fish, S.S., Harrach, B., Wellehan, J.F.X., 2014. A novel siadenovirus detected in the kidneys and liver of Gouldian finches (*Erythura gouldiae*). Vet. Microbiol. 172, 35–43. https://doi.org/10.1016/j.vetmic.2014.04.006.

Jumper, J., Evans, R., Pritzel, A., Green, T., Figurnov, M., Ronneberger, O., Tunyasuvunakool, K., Bates, R., Žídek, A., Potapenko, A., Bridgland, A., Meyer, C., Kohl, S.A.A., Ballard, A.J., Cowie, A., Romera-Paredes, B., Nikolov, S., Jain, R., Adler, J., Back, T., Petersen, S., Reiman, D., Clancy, E., Zielinski, M., Steinegger, M., Pacholska, M., Berghammer, T., Bodenstein, S., Silver, D., Vinyals, O., Senior, A.W., Kavukcuoglu, K., Kohli, P., Hassabis, D., 2021. Highly accurate protein structure prediction with AlphaFold. Nature 596, 583–589. https://doi.org/10.1038/s41586-021-03819-2.

Kaján, G.L., 2016. Poultry adenoviruses. In: Liu, D. (Ed.), Molecular Detection of Animal Viral Pathogens. CRC Press, Boca Raton, pp. 735–746.

Kaján, G.L., Sameti, S., Benkő, M., 2011. Partial sequence of the DNA-dependent DNA polymerase gene of fowl adenoviruses: a reference panel for a general diagnostic PCR in poultry. Acta Vet. Hung. 59, 279–285. https://doi.org/10.1556/AVet.2011.006.

Kaján, G.L., Doszpoly, A., Tarján, Z.L., Vidovszky, M., Papp, T., 2020. Virus–host coevolution with a focus on animal and human DNA viruses. J. Mol. Evol. 88, 41–56. https://doi.org/10.1007/s00239-019-09913-4.

Katoh, K., Standley, D.M., 2013. MAFFT multiple sequence alignment software version 7: improvements in performance and usability. Mol. Biol. Evol. 30, 772–780. https://doi.org/10.1093/molbev/mst010.

Kearse, M.G., Wilusz, J.E., 2017. Non-AUG translation: a new start for protein synthesis in eukaryotes. Genes Dev. 31, 1717–1731. https://doi.org/10.1101/GAD.305250.117.

Kovács, E.R., Benkő, M., 2011. Complete sequence of raptor adenovirus 1 confirms the characteristic genome organization of siadenoviruses. Infect. Genet. Evol. 11, 1058–1065. https://doi.org/10.1016/j.meegid.2011.03.021.

Kovács, E.R., Jánoska, M., Dán, Á., Harrach, B., Benkő, M., 2010. Recognition and partial genome characterization by non-specific DNA amplification and PCR of a new siadenovirus species in a sample originating from *Parus major*, a great tit. J. Virol. Methods 163, 262–268. https://doi.org/10.1016/j.jviromet.2009.10.007.

Kozlov, A.M., Darriba, D., Flouri, T., Morel, B., Stamatakis, A., 2019. RAxML-NG: a fast, scalable and user-friendly tool for maximum likelihood phylogenetic inference. Bioinformatics 35, 4453–4455. https://doi.org/10.1093/bioinformatics/btz305.

Kumar, S., Stecher, G., Tamura, K., 2016. MEGA7: Molecular Evolutionary Genetics Analysis version 7.0 for bigger datasets. Mol. Biol. Evol. 33, 1870–1874. https://doi.org/10.1093/molbev/msw054.

Lee, S.Y., Kim, J.H., Park, Y.M., Shin, O.S., Kim, H., Choi, H.G., Song, J.W., 2014. A novel adenovirus in chinstrap penguins (*Pygoscelis antarctica*) in Antarctica. Viruses 6, 2052–2061. https://doi.org/10.3390/v6052052.

Lemoine, F., Domelevo Entfellner, J.-B., Wilkinson, E., Correia, D., Dávila Felipe, M., De Oliveira, T., Gascuel, O., 2018. Renewing Felsenstein's phylogenetic bootstrap in the era of big data. Nature 556, 452–456. https://doi.org/10.1038/s41586-018-0043-0.

Lenman, A., Liaci, A.M., Liu, Y., Årdahl, C., Rajan, A., Nilsson, E., Bradford, W., Kaeshammer, L., Jones, M.S., Frängsmyr, L., Feizi, T., Stehle, T., Arnberg, N., 2015. Human adenovirus 52 uses sialic acid-containing glycoproteins and the coxsackie and adenovirus receptor for binding to target cells. PLoS Pathog. 11, e1004657 https://doi.org/10.1371/journal.ppat.1004657.

Lenman, A., Manuel Liaci, A., Liu, Y., Frängsmyr, L., Frank, M., Blaum, B.S., Chai, W., Podgorski, I.I., Harrach, B., Benko, M., Feizi, T., Stehle, T., Arnberg, N., 2018. Polysialic acid is a cellular receptor for human adenovirus 52. Proc. Natl. Acad. Sci. U. S. A. 115, E4264–E42736. https://doi.org/10.1073/PNAS.1716900115/-/DCSUPPLEMENTAL.

Merbach, S., Peters, M., Kilwinski, J., Reckling, D., 2019. Suttonella ornithocola-associated mortality in tits in Germany. Berl. Munch. Tierarztl. Wochenschr. 132, 459–463. https://doi.org/10.2376/0005-9366-18065.

Muhire, B.M., Varsani, A., Martin, D.P., 2014. SDT: a virus classification tool based on pairwise sequence alignment and identity calculation. PLoS One 9, e108277. https://doi.org/10.1371/journal.pone.0108277.

Pantchev, A., Sting, R., Bauerfeind, R., Tyczka, J., Sachse, K., 2009. New real-time PCR tests for species-specific detection of Chlamydophila psittaci and Chlamydophila abortus from tissue samples. Vet. J. 181, 145–150. https://doi.org/10.1016/J.TVJL.2008.02.025.

Park, Y.M., Kim, J.-H., Gu, S.H., Lee, S.Y., Lee, M.-G., Kang, Y.K., Kang, S.-H., Kim, H.J., Song, J.-W., 2012. Full genome analysis of a novel adenovirus from the south polar skua (*Catharacta maccormicki*) in Antarctica. Virology 422, 144–150. https://doi.org/10.1016/j.virol.2011.10.008.

Phalen, D.N., Agius, J., Vaz, F.F., Eden, J.-S., Setyo, L.C., Donahoe, S., 2019. A survey of a mixed species aviary provides new insights into the pathogenicity, diversity, evolution, host range, and distribution of psittacine and passerine adenoviruses. Avian Pathol. 48, 437–443. https://doi.org/10.1080/03079457.2019.1617835.

Pries, F., Kingma, J., Janssen, D.B., 1995. Activation of an Asp-124–>Asn mutant of haloalkane dehalogenase by hydrolytic deamidation of asparagine. FEBS Lett. 358, 171–174. https://doi.org/10.1016/0014-5793(94)01420-6.

Rinder, M., Schmitz, A., Baas, N., Korbel, R., 2020. Molecular identification of novel and genetically diverse adenoviruses in Passeriform birds. Virus Genes 56, 316–324. https://doi.org/10.1007/s11262-020-01739-3.

Sarker, S., 2021. Metagenomic detection and characterisation of multiple viruses in apparently healthy Australian Neophema birds. Sci. Rep. 11, 20915. https://doi.org/10.1038/S41598-021-00440-1.

Schrödinger, L., 2021. Schrödinger Suite. Schrödinger, LLC, New York, NY.

Surphlis, A.C., Dill-Okubo, J.A., Harrach, B., Waltzek, T., Subramaniam, K., 2022. Genomic characterization of psittacine adenovirus 2, a siadenovirus identified in a moribund African grey parrot (*Psittacus erithacus*). Arch. Virol. 167, 911–916. https://doi.org/10.1007/s00705-021-05341-2.

Sutherland, M., Sarker, S., Vaz, P.K., Legione, A.R., Devlin, J.M., Macwhirter, P.L., Whiteley, P.L., Raidal, S.R., 2019. Disease surveillance in wild Victorian cacatuids reveals co-infection with multiple agents and detection of novel avian viruses. Vet. Microbiol. 235, 257–264. https://doi.org/10.1016/j.vetmic.2019.07.012.

Vaz, F.F., Raso, T.F., Agius, J.E., Hunt, T., Leishman, A., Eden, J.-S., Phalen, D.N., 2020. Opportunistic sampling of wild native and invasive birds reveals a rich diversity of adenoviruses in Australia. Virus Evol. 6, veaa024. https://doi.org/10.1093/ve/veaa024.

Wellehan, J.F.X., Johnson, A.J., Harrach, B., Benkő, M., Pessier, A.P., Johnson, C.M., Garner, M.M., Childress, A., Jacobson, E.R., 2004. Detection and analysis of six lizard adenoviruses by consensus primer PCR provides further evidence of a reptilian origin for the atadenoviruses. J. Virol. 78, 13366–13369. https://doi.org/10.1128/jvi.78.23.13366-13369.2004.

Withers, S.G., Rupitz, K., Trimbur, D., Warren, R.A.J., 1992. Mechanistic consequences of mutation of the active site nucleophile Glu 358 in Agrobacterium beta-glucosidase. Biochemistry 31, 9979–9985. https://doi.org/10.1021/BI00156A017.

Wu, K., Orozco, D., Hearing, P., 2012. The adenovirus L4-22K protein is multifunctional and is an integral component of crucial aspects of infection. J. Virol. 86, 10474–10483. https://doi.org/10.1128/JVI.01463-12.

Wu, K., Guimet, D., Hearing, P., 2013. The adenovirus L4-33K protein regulates both late gene expression patterns and viral DNA packaging. J. Virol. 87, 6739–6747. https://doi.org/10.1128/JVI.00652-13.

Zaramela, L.S., Martino, C., Alisson-Silva, F., Rees, S.D., Diaz, S.L., Chuzel, L., Ganatra, M.B., Taron, C.H., Secrest, P., Zuñiga, C., Huang, J., Siegel, D., Chang, G., Varki, A., Zengler, K., 2019. Gut bacteria responding to dietary change encode sialidases that exhibit preference for red meat-associated carbohydrates. Nat. Microbiol. 4, 2082–2089. https://doi.org/10.1038/s41564-019-0564-9.

Ziegler, U., Bergmann, F., Fischer, D., Müller, K., Holicki, C.M., Sadeghi, B., Sieg, M., Keller, M., Schwehn, R., Reuschel, M., Fischer, L., Krone, O., Rinder, M., Schütte, K., Schmidt, V., Eiden, M., Fast, C., Günther, A., Globig, A., Conraths, F.J., Staubach, C., Brandes, F., Lierz, M., Korbel, R., Vahlenkamp, T.W., Groschup, M.H., 2022. Spread of West Nile virus and Usutu virus in the German bird population, 2019–2020. Microorganisms 10, 807. https://doi.org/10.3390/microorganisms10040807.